Redox Biology 76 (2024) 103329

Contents lists available at ScienceDirect

Redox Biology

journal homepage: www.elsevier.com/locate/redox

Role of Mitofusin 1 in mediating reactive oxygen species in alveolar macrophages during *Streptococcus pneumoniae*

David Thomas [a,b], Jianjun Yang [a], Soo Jung Cho [a,b], Heather Stout-Delgado [a,*]

[a] Division of Pulmonary and Critical Care Medicine, Joan and Sanford I. Weill Department of Medicine, Weill Cornell Medicine, USA
[b] New York-Presbyterian Hospital, New York, NY, USA

A B S T R A C T

Alveolar macrophages (AM) are key effectors of the immune response and are essential for host responses to *S. pneumoniae*. Mitochondria are highly dynamic organelles whose function aids in regulating the cell cycle, innate immunity, autophagy, redox signaling, calcium homeostasis, and mitochondrial quality control in AM. In response to cellular stress, mitochondria can engage in stress-induced mitochondrial hyperfusion (SIMH). The current study aimed to investigate the role of Mfn1 on mitochondrial control of reactive oxygen species (ROS) in AMs and the role of Mfn1 deficiency on immune responses to *S. pneumoniae*. Compared to $Mfn1^{FloxCre-}$ controls, there were distinct histological differences in lung tissue collected from $Mfn1^{Floxed;\ CreLysM}$ mice, with less injury and inflammation observed in mice with Mfn1 deficient myeloid cells. There was a significant decrease in lipid peroxidation and ROS production in Mfn1 deficient AM that was associated with increased superoxide dismutase (SOD) and antioxidant activity. Our findings demonstrate that Mfn1 deficiency in myeloid cells decreased inflammation and lung tissue injury during *S. pneumoniae* infection.

1. Introduction

Acute Respiratory Distress Syndrome (ARDS) is a severe form of acute lung injury (ALI) defined by poor oxygenation, inflammation, increased presence of pulmonary infiltrates, and diffuse alveolar damage. Bacterial pneumonia, for which *Streptococcus pneumoniae* (*S. pneumoniae*) is a frequently responsible pathogen, can contribute to ARDS development [1].

Resident alveolar macrophages (AM) are innate immune cells in the airways. Alveolar macrophages play an intricate role in lung tissue homeostasis and are critical effectors of the host immune responses against microbes, such as *S. pneumoniae* [2]. Due to the presence of surfactants, AMs are essential in maintaining balance within the lipid-rich environment of the lung. Excessive oxidation of AM can lead to cell death and the release of cytotoxic mediators that can further initiate inflammatory signaling cascades and augment inflammation. Reactive oxygen species, specifically those generated by mitochondria, have been previously shown to play an essential role in mediating AM responses [3].

Mitochondria are highly dynamic organelles that play a crucial role in the cell cycle, innate immunity, autophagy, redox signaling, calcium homeostasis, and mitochondrial quality control in AM. Communication between the mitochondria, nucleus, and cytosol is crucial for maintaining proper mitochondrial function and cellular homeostasis [4]. Mitochondria are dynamic organelles that undergo cycles of fission and fusion, essential in maintaining mitochondrial structural integrity, regulating organelle quality control, and sustaining inter-organellular connections. While mitochondrial fission divides one mitochondrion into two, mitochondrial fusion is the union of two mitochondria into elongated structures. Fusion of the outer mitochondrial membrane (OMM) is mediated by mitofusins (Mfn) 1 and 2, followed by optic atrophy 1 (Opa1) mediated inner mitochondrial membrane (IMM) fusion. In response to cellular stress, mitochondria can experience stress-induced mitochondrial hyperfusion (SIMH) [5–7]. When cells are subjected to moderate levels of mitochondrial or endoplasmic reticulum (ER) stress, mitochondria can fuse into an interconnected reticulum, a hallmark feature of SIMH [7]. SIMH optimizes ATP production and OXPHOS signaling to mitigate cellular stress and help cells overcome transient reversible metabolic insults [7]. Unfortunately, prolonged and sustained stress can reverse SIMH and lead to mitochondrial fragmentation. Previous work has demonstrated that SIMH requires Opa1, Mfn1, and stomatin-like protein 2 (Slp-2), independent of Mfn2 [7]. In addition, degradation or loss of dynamin-related protein 1 (Drp1) can result in decreased fission and increased mitochondrial hyperfusion [8,9]. In culture systems, SIMH induction can serve as a mechanism to protect stressed cells against apoptosis and mitophagy [10,11]. While mitochondrial hyperfusion can alleviate cellular stress, little is currently

* Corresponding author. Weill Cornell Medicine, Joan and Sanford I. Weill Department of Medicine, Division of Pulmonary and Critical Care, 1300 York Avenue, Box 96, New York, NY, 10065, USA.
E-mail address: hes2019@med.cornell.edu (H. Stout-Delgado).

https://doi.org/10.1016/j.redox.2024.103329
Received 13 August 2024; Accepted 25 August 2024
Available online 27 August 2024

known regarding Mfn1 or the role of Mfn1-mediated SIMH in modulating host defense against *S. pneumoniae*.

Previous work has demonstrated that infection with HIV-1 or challenge with viral dsRNAs can contribute to SIMH induction of mitochondrial antiviral signaling (MAVS) [12]. In addition to modulating SIMH, Mfn1 can directly associate with MAVS on the OMM to positively regulate retinoic acid-inducible gene I (*Rig-I*)-like Receptor (RLR) mediated innate antiviral responses in fibroblasts [13]. Experimental studies have illustrated the critical role of Mfn1 in IFN production in human monocytic macrophages in response to cytomegalovirus infection [14]. In these models, the knockdown of Mfn1 abrogated the virus-induced redistribution of MAVS and IFN production [13,14]. Despite these findings, little is currently known regarding the role of Mfn1-mediated SIMH induction in modulating host defense against *S. pneumoniae*.

Results from the current study demonstrated that Mfn1 deficiency resulted in a significant decrease in reactive oxygen species (ROS) production that was associated with increased superoxide dismutase (SOD) activity and decreased lipid peroxidation. Our findings demonstrate that Mfn1 can modulate host immune responses to *S. pneumoniae* infection.

2. Results

2.1. Decreased Cellular recruitment and lung tissue injury in Mfn1 deficient mice

During *S. pneumoniae*, a notable increase in *Mfn1* expression was detected in alveolar macrophages 24 h post-infection (Supplemental Fig. 1). To determine if Mfn1 was necessary for mediating host responses to *S. pneumoniae*, age-matched wild-type ($Mfn1^{FloxCre-}$) and myeloid deficient Mfn1 ($Mfn1^{Floxed;\ CreLysM}$) mice were instilled with 1×10^5 CFU of *S. pneumoniae* before lung tissue collection. In the absence of myeloid-specific Mfn1 expression, tissue injury and cellular recruitment to the lung were reduced 72 h post-infection (Fig. 1A). To confirm these results, we quantified cellularity in bronchoalveolar lavage (BAL) collected from $Mfn1^{FloxCre-}$ and $Mfn1^{Floxed;\ CreLysM}$ at 24 and 72 h post-infection and observed a significant reduction in cellular infiltration in BAL collected from $Mfn1^{Floxed;\ CreLysM}$ mice (Fig. 1B). We examined the role of myeloid Mfn1 expression on pulmonary edema and lung permeability. By 72 h post-infection, mice deficient in myeloid Mfn1 expression had significantly less pulmonary edema and lower lung permeability when compared to wild-type controls (Fig. 1C–D). In addition, by 24 h post-infection, a significant increase in bacterial clearance was observed in the lung of $Mfn1^{Floxed;\ CreLysM}$ mice (Fig. 1E).

Due to the potential of the LysM-Cre system to target myeloid cells as well as a subset of lung epithelial cells, we first examined Mfn1 expression in alveolar macrophages (AM) and alveolar epithelial cells (AEC) isolated from wild-type ($Mfn1^{FloxCre}$) and Mfn1 deficient ($Mfn1^{Floxed;\ CreLysM}$) mice [15]. Compared to wild-type AM, there was a significant decrease in Mfn1 expression in AM isolated from LysM-Cre^{+} mice (Supplemental Fig. 2A. In addition, while a reduction in Mfn1 expression was observed in AEC isolated from LysM-Cre^{+} mice, the levels were not significantly different from those observed in wild-type LysM-Cre^{-} mice (Supplemental Fig. 2B). As a decrease in Mfn1 expression might result in changes to Mfn2 expression, we assessed gene levels in Mfn1 deficient mice. Compared to wild-type, AM and AEC isolated from wild-type and LysM-Cre^{+} mice had similar *Mfn2* gene expression (Supplemental Fig. 2C).

2.2. Decreased Chemokine and Cytokine Expression in Lung and Alveolar Macrophages isolated from Mfn1 deficient mice

We assessed inflammatory protein levels in the lung at baseline and during infection to investigate if immune signaling and cytokine production were altered in Mfn1-deficient myeloid cells. When compared to wild-type, lung tissue isolated from myeloid deficient Mfn1 mice had

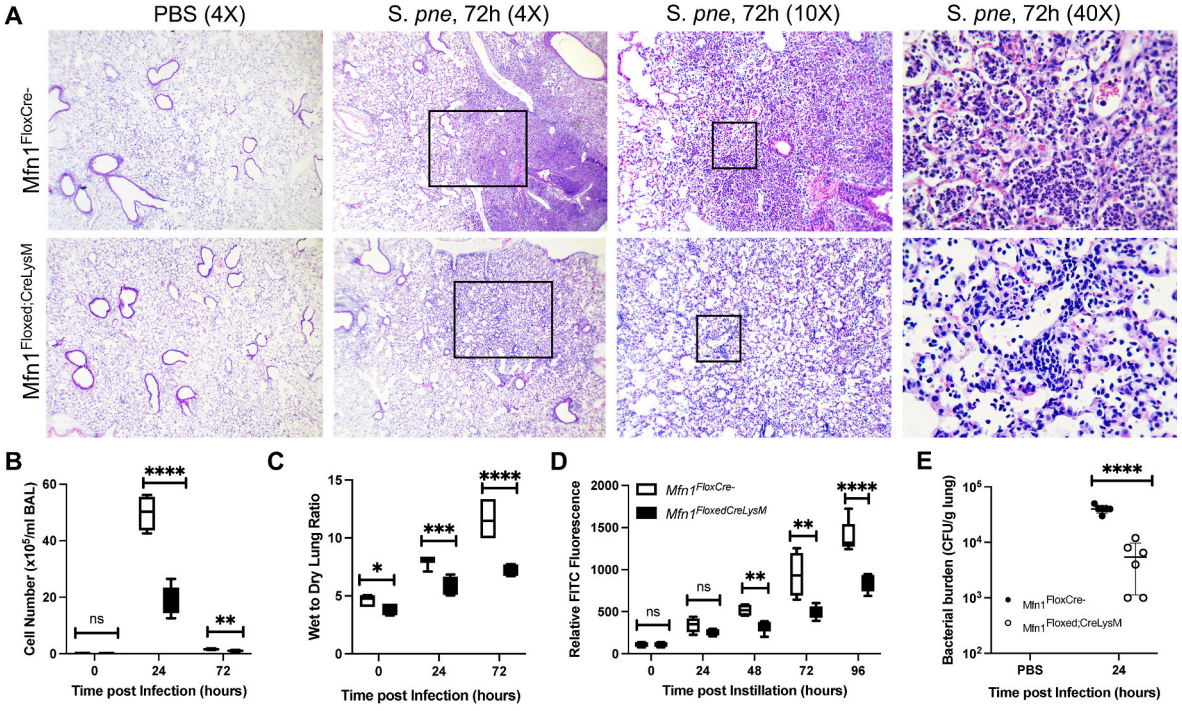

Fig. 1. *Decreased Cellular Recruitment and Lung Tissue Injury in Mfn1 Deficient Mice*. Wild-type ($Mfn1^{FloxCre-}$) and myeloid deficient Mfn1 ($Mfn1^{Floxed;CreLysM}$) mice were infected with *S. pneumoniae*. (**A**) At 72 h of infection, lung tissue was collected. Representative hematoxylin and eosin-stained photomicrographs are shown (magnification of×4, × 10 and × 40). (**B**) BAL was isolated and the total cell number was quantified. (**C**) The wet-to-dry ratio of lung tissue was assessed in wild-type and Mfn1-deficient mice. (**D**) Fluorescence in plasma was assessed 1-h post-instillation. (**E**) CFU was assessed in lung tissue collected. N = 5–10 per group, ns: not significant, $^{*}p < 0.05$, $^{**}p < 0.01$, $^{***}p < 0.001$, $^{****}p < 0.0001$. Results were repeated at least twice. Statistical significance was determined for results from independent biological replicates.

significantly decreased expression of chemokine (C–C motif) ligand (Ccl) 2, Ccl3/4, Ccl19, granulocyte-macrophage colony-stimulating factor (GM-CSF), interferon (IFN)-g, interleukin (IL)-6, IL-7, and IL-15 (Fig. 2A–B). Interestingly, in the absence of Mfn1, increased chitinase 3-like 1 and endostatin protein levels were observed 24 h post-infection (Fig. 2C). We next investigated the impact of Mfn1 deficiency on AM-mediated immune responses to direct infection with *S. pneumoniae*. Mfn1 deficient AM displayed significantly lower gene expression of C-X-C motif chemokine ligand (*Cxcl*)1, *Cxcl3, IL-1b*, and *Ifnb1* than wild-type AM (Fig. 2D–G).

As phagocytosis of *S. pneumoniae* by AMs plays a critical role in mediating bacterial clearance, we next investigated the impact of Mfn1 on phagocytic gene expression and function. Briefly, freshly isolated AMs from naïve wild-type ($Mfn1^{FloxCre-}$) and Mfn1 deficient ($Mfn1^{Floxed;CreLysM}$) mice were cultured with media alone or with *S. pneumoniae* (MOI = 10) for 30 min to allow bacteria to bind. AMs were subsequently incubated for 60 min before adding gentamicin to allow bacterial uptake. AMs were subsequently cultured for 30–120 min or 1–4 h before RNA isolation or CFU quantification, respectively. When compared to wild-type, despite a similar declining trend in expression, Mfn1 deficient AM had significantly increased phagocytic receptor expression, as demonstrated by elevated carcinoembryonic antigen-related cell adhesion molecule 3 (*Ceacam3*) and GULP PTB domain containing engulfment adaptor 1 (*Gulp1*), at 30 and 60 min of infection (Fig. 3A–B). Similarly, we detected enhanced macrophage receptor with collagenous structure (*Marco*) and myeloid differentiation primary response 88 (*Myd88*) expression in Mfn1 deficient AM when compared to wild-type (Fig. 3C–D). Interestingly, expression of lipid scavenger receptors, such as scavenger receptor class B type 1 (*Scarb1*), significantly decreased at 60 and 120 min of *S. pneumoniae* infection in Mfn1 deficient AM compared to wild-type (Fig. 3E). To determine the functional outcome of Mfn1 deficiency in AM on *S. pneumoniae*, we assessed bacterial clearance at select time points of infection. In the absence of Mfn1, *S. pneumoniae* clearance was increased (Fig. 3F).

2.3. *Mfn1 is necessary for S. pneumoniae induced SIMH in AM*

Given the role of Mfn1 in mediating SIMH, we investigated changes in mitochondrial structure and SIMH formation in response to *S. pneumoniae*. Alveolar macrophages were isolated from naïve wild-type ($Mfn1^{FloxCre-}$) and Mfn1 deficient ($Mfn1^{Floxed;\ CreLysM}$) mice and cultured with media alone or media containing *S. pneumoniae* (MOI = 10). AMs were cultured with *S. pneumoniae* before fixation and processing for transmission electron microscopy (TEM). In the presence of Mfn1, increased SIMH was observed in alveolar macrophages infected with *S. pneumoniae* (Fig. 4A). In the absence of Mfn1, there were distinct differences in mitochondrial morphology at baseline and during *S. pneumoniae* (Fig. 4B). Notably, SIMH formation was absent, and there was enhanced loss of mitochondrial integrity and increased mitophagy in Mfn1 deficient AM (Fig. 4B). Mitochondrial damage can increase oxidative stress and cellular responsiveness to pathogenic stimuli. To determine the potential role of Mfn1 in mediating oxidative phosphorylation (OXPHOS), we isolated protein from wild-type and Mfn1 deficient AM at select time points of *S. pneumoniae* infection. We assessed the expression of complex I–V genes. In the absence of Mfn1, a decline in complex protein expression was observed in response to *S. pneumoniae* (Fig. 4C).

2.4. *Decreased Mitochondrial Bioenergetics in Mfn1 deficient macrophages*

As SIMH optimizes ATP production and OXPHOS signaling to mitigate cellular stress and help cells overcome transient reversible metabolic insults, we evaluated the impact of Mfn1 deficiency on mitochondrial bioenergetics. Previous work has demonstrated that Mfn1 overexpression can increase mitochondrial basal respiration, ATP synthesis, and proton leak in pulmonary endothelial cells [16]. We evaluated the impact of Mfn1 deficiency on the oxygen consumption rate (OCR) in bone marrow-derived (BMM) (Fig. 5A) and alveolar (Fig. 5B) macrophages. Compared to wild-type, Mfn1 deficient macrophages had decreased basal respiration, ATP synthesis, maximum respiratory

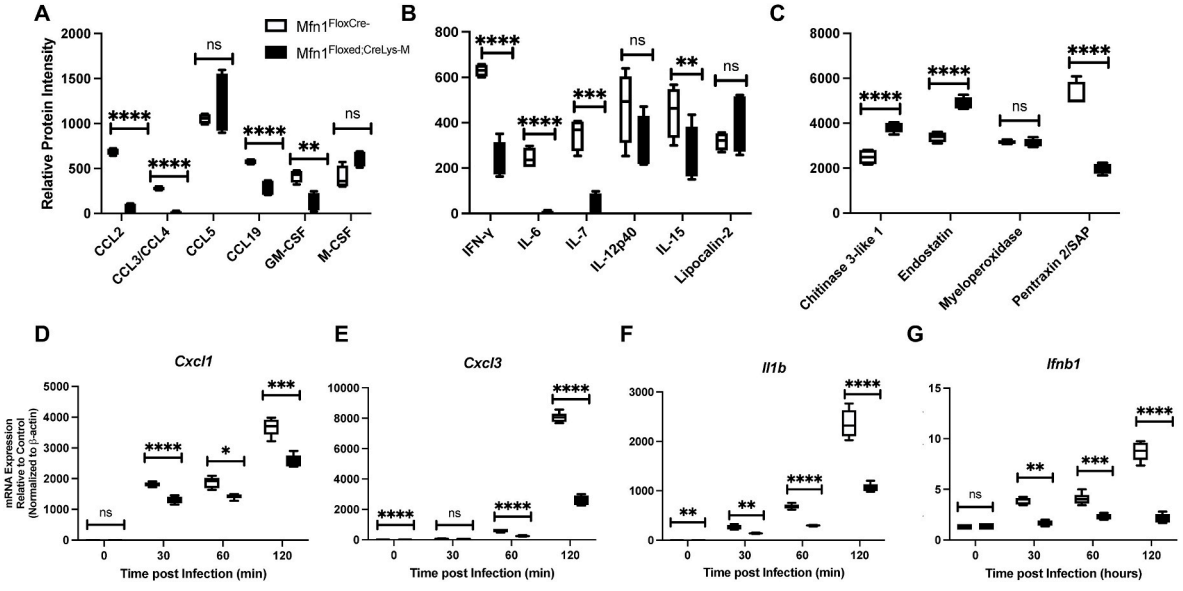

Fig. 2. *Decreased Chemokine and Cytokine Expression in Lung and Alveolar Macrophages isolated from Mfn1 Deficient Mice.* (**A-C**) Wild-type ($Mfn1^{FloxCre-}$) and myeloid deficient Mfn1 ($Mfn1^{Floxed;CreLysM}$) mice were intranasally instilled with 1×10^5 CFU of *S. pneumoniae* and lung tissue was collected at 24 h post-infection. Production of (**A**) CCL2, CCL3/CCL4, CCL5, CCL19, GM-CSF, and M-CSF, (**B**) IFN-g, IL-6, IL-7, IL-12p40, IL-15, and lipocalin-2 (**C**) chitinase 3-like 1, endostatin, myeloperoxidase, and pentraxin 2 were quantified in lung homogenates. N = 3 samples per group run in duplicate. (**D-G**) Alveolar macrophages were isolated from naïve wild-type and myeloid-deficient Mfn1 mice before infection with *S. pneumoniae* (MOI = 10) for 30–120 min. Expression of (**D**) *Cxcl1*, (**E**) *Cxcl3*, (**F**) *Il1b*, and (**G**) *Ifnb1* were quantified by real-time PCR. Statistical significance was determined for results from independent biological replicates. N = 5–10 samples per group, $*p < 0.05$, $**p < 0.01$, $***p < 0.001$, $****p < 0.0001$. Results were repeated at least three times. Representative results are shown.

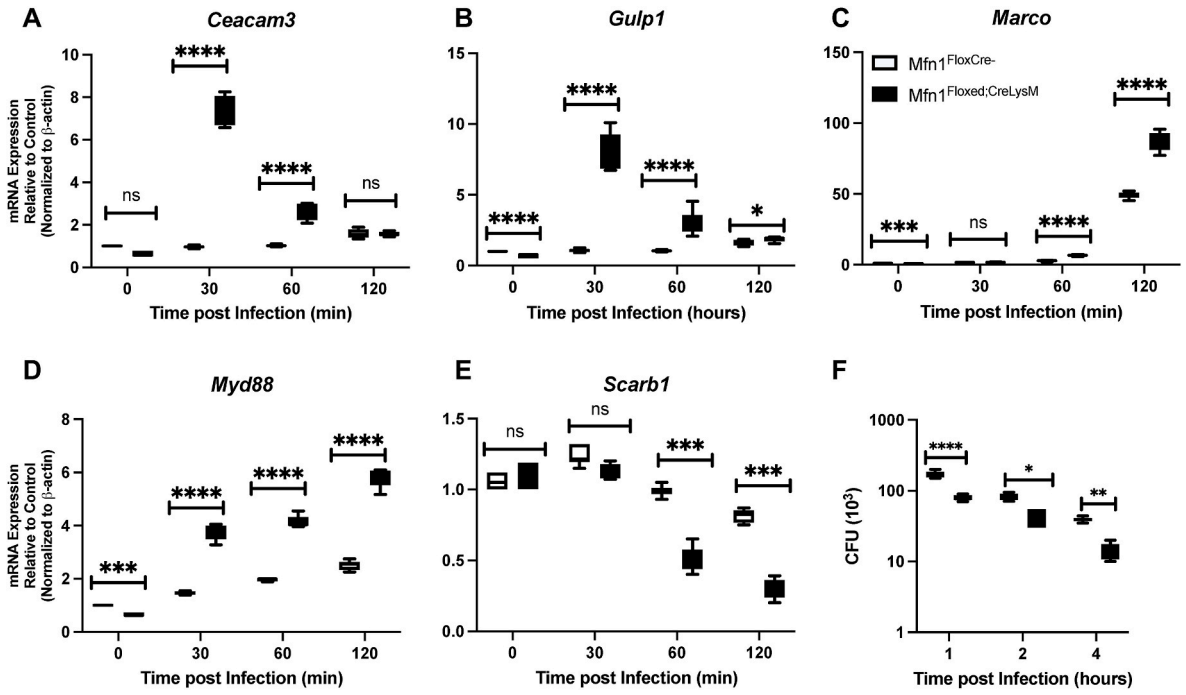

Fig. 3. *Altered Phagocyte Receptor Expression in Mfn1 Deficient AM is Associated with Increased S. pneumoniae Clearance.* Alveolar macrophages were isolated from naïve wild-type ($Mfn1^{FloxCre-}$) and myeloid deficient Mfn1 ($Mfn1^{Floxed;CreLysM}$) mice before infection with *S. pneumoniae* (MOI = 10) for 30–120 min. Expression of (**A**) *Ceacam3*, (**B**) *Gulp1*, (**C**) *Marco*, (**D**) *Myd88*, and (**E**) *Scarb1* were quantified by real-time PCR. (**F**) Cells were collected and lysed before CFU quantification. Statistical significance was determined for results from independent biological replicates. N = 5–10 samples per group. ns: not significant, $*p < 0.05$, $**p < 0.01$, $***p < 0.001$, $****p < 0.0001$. Results were repeated at least three times. Representative results are shown.

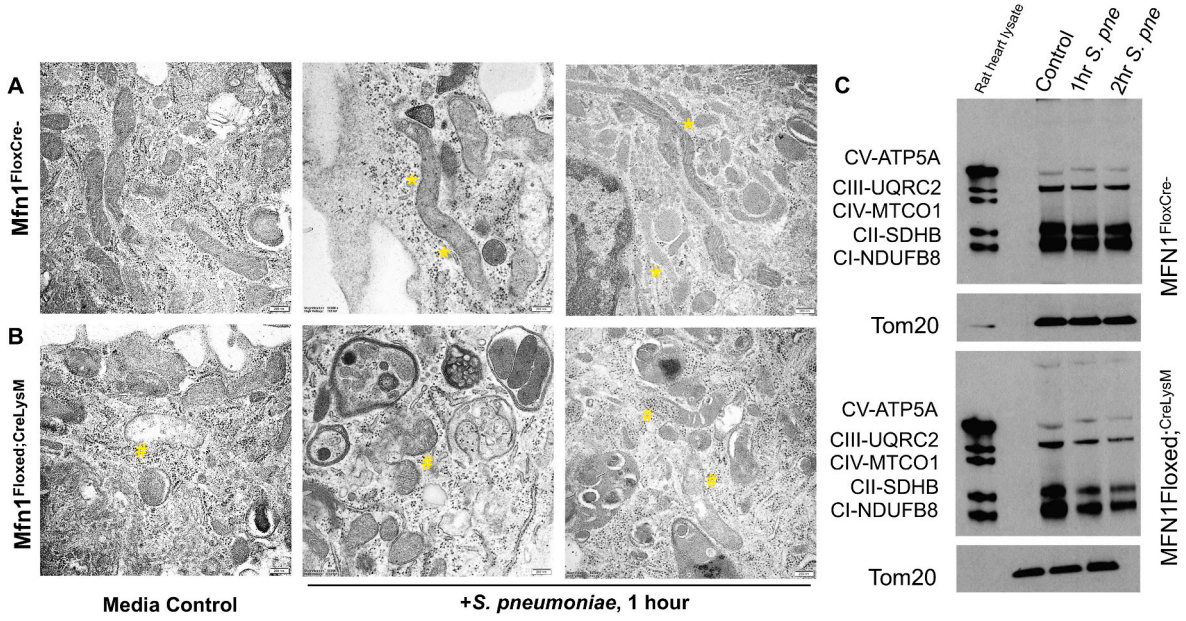

Fig. 4. *Mfn1 is necessary for S. pneumoniae Induced SIMH.* Alveolar macrophages were isolated from naïve wild-type ($Mfn1^{FloxCre-}$) and myeloid deficient Mfn1 ($Mfn1^{Floxed;CreLysM}$) mice before infection with *S. pneumoniae* (MOI = 10). Representative TEM images of media control or *S. pneumoniae* infected (1 h) (**A**) wild-type and (**B**) Mfn1 deficient alveolar macrophages. Bar = 200 nm. (*) areas of SIMH and (#) mitochondrial rupture. (**C**) Protein was collected from control and *S. pneumoniae*-infected macrophages and complex I–V expression was assessed by western blot. N = 5 per group were evaluated. Results were repeated at least three times. Representative results are shown.

capacity, and proton leak (Fig. 5A–B).

2.5. Decreased Cellular and Mitochondrial ROS Production in Mfn1 deficient AM

Due to changes in OXPHOS expression in the absence of Mfn1, we evaluated if ROS levels might also be altered during *S. pneumoniae*

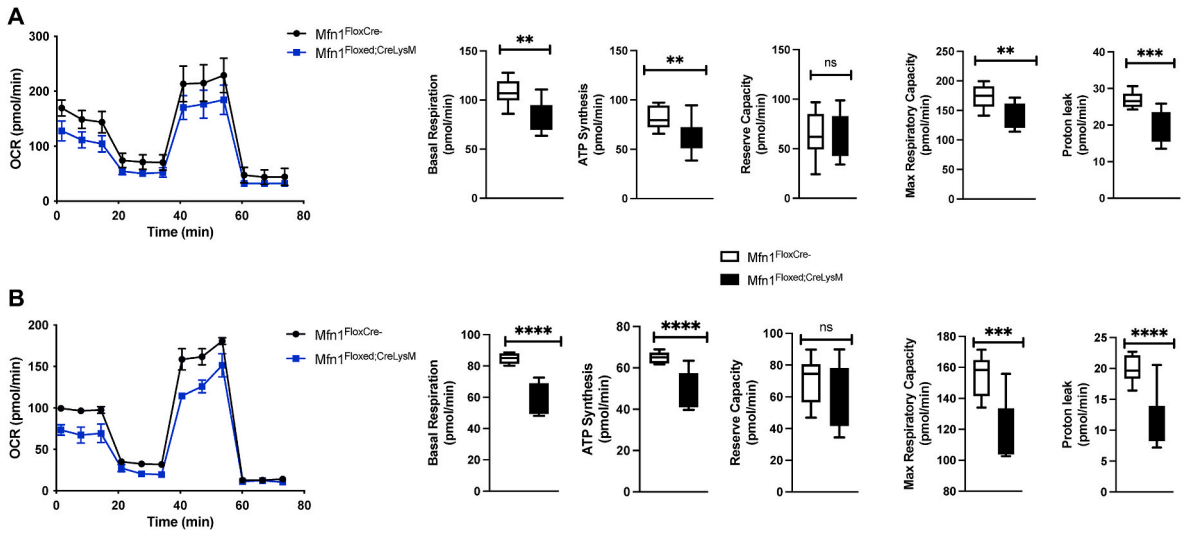

Fig. 5. *Decreased Mitochondrial Bioenergetics in Mfn1 Deficient Macrophages*. Bone-marrow derived and alveolar macrophages were isolated from naïve wild-type ($Mfn1^{FloxCre-}$) and myeloid deficient Mfn1 ($Mfn1^{Floxed;CreLysM}$) mice and plated overnight prior to Seahorse analysis. Oxygen consumption rate (OCR) was assessed in (A) bone marrow derived and (B) alveolar macrophages. Basal respiration, ATP synthesis, reserve capacity, maximum respiratory capacity, and proton leak were quantified using previously established methods [30]. Statistical significance was determined for results from independent biological replicates. N = 3 samples per group. ns: not significant, $^{**}p < 0.01$, $^{***}p < 0.001$, $^{****}p < 0.0001$. Results were repeated at least three times. Representative results are shown.

infection. To examine cellular ROS generation, freshly isolated wild-type, and Mfn1 deficient AM were co-cultured with *S. pneumoniae* (MOI = 10) for 60 min post-binding and gentamicin treatment. At the end of incubation, cells were treated with ROS staining buffer containing dihydroethidium (DHE; 5 mM), and fluorescence was measured. While cellular ROS levels increased in both groups, significantly less ROS was detected in Mfn1 deficient AM (Fig. 6A). Next, we quantified whether the observed difference in cellular ROS was due to changes in mitochondrial ROS. To this extent, wild-type and Mfn1 deficient AM were pre-treated with a mitochondrial-specific ROS detection reagent before incubation with *S. pneumoniae* (1 h). Mitochondrial ROS levels in Mfn1 deficient AM were significantly decreased at baseline and in response to incubation with antimycin A (100 mM) (Fig. 6B). Similarly, in response to *S. pneumoniae*, there was significantly increased mitochondrial ROS present in wild-type AM compared to Mfn1 deficient AM (Fig. 6B).

Hydrogen peroxide is a ROS moiety produced during numerous cellular responses and can function as a cytotoxic agent generated by phagocytic immune cells during the engulfment of microbes. Importantly, extracellular hydrogen peroxide can induce bacterial oxidative damage. To determine if Mfn1 expression might contribute to changes in hydrogen peroxide production, wild-type and Mfn1 deficient macrophages were cultured overnight with media alone or media containing *S. pneumoniae*. At 24 h, hydrogen peroxide levels were quantified using 10-acetyl-3,7-dihyroxyphenoxazine (ADAP), a highly sensitive and stable probe for hydrogen peroxide. Compared to the wild-type, there was a significant elevation in hydrogen peroxide in Mfn1 deficient macrophages in response to *S. pneumoniae* (Fig. 6C).

2.6. Enhanced SOD Activity in Mfn1 deficient AM during S. pneumoniae infection

Superoxide dismutases (SODs) catalyze the dismutation of superoxide anions to molecular oxygen and hydrogen peroxide. Superoxides are present in the cytoplasm and extracellular space, and the presence of SODs is crucial to metabolizing cellular ROS. Given the importance of SODs in the generation, we next examined if increased hydrogen peroxide production by Mfn1 deficient macrophages might be due to alterations in SOD activity. To this extent, we examined SOD activity in plasma and bronchoalveolar lavage (BAL) samples isolated from control (PBS) and *S. pneumoniae-infected* wild-type and Mfn1 deficient mice at 24 h post-instillation. In plasma samples, significantly less SOD activity was detected in mice with Mfn1 deficient myeloid cells ($Mfn1^{Floxed;CreLysM}$) at baseline and during *S. pneumoniae* infection (Fig. 7A). We next investigated SOD activity in BAL isolated from wild-type and Mfn1 deficient mice. In response to *S. pneumoniae*, there was significantly higher SOD activity in myeloid Mfn1 deficient BAL when compared to

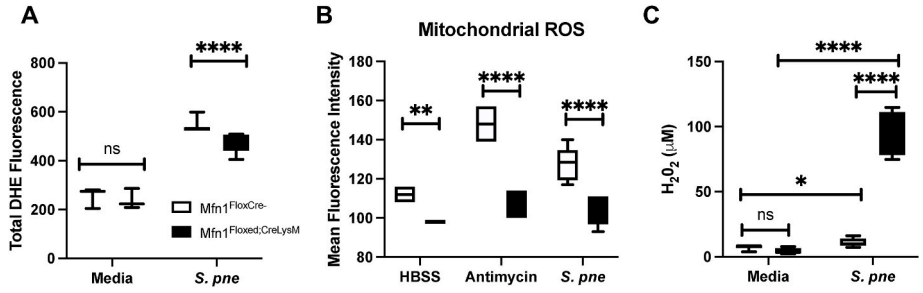

Fig. 6. *Decreased Cellular and Mitochondrial ROS Production in Mfn1 Deficient AM.* Alveolar macrophages were isolated from naïve wild-type ($Mfn1^{FloxCre-}$) and myeloid deficient Mfn1 ($Mfn1^{Floxed;CreLysM}$) mice *before* infection with *S. pneumoniae* (MOI = 10) for 1 h *and* quantification of (**A**) dihydroethidium fluorescence (cellular ROS) or (**B**) mitochondrial ROS. (**C**) Bone marrow-derived macrophages were cultured with *S. pneumoniae* (MOI = 10, 18–24 h) before quantification of H_2O_2 levels in cell culture media. Statistical significance was determined for results from independent biological replicates. N = 5–10 samples per group. ns: not significant, $^{*}p < 0.05$, $^{**}p < 0.01$, $^{****}p < 0.0001$. Results were repeated at least three times. Representative results are shown.

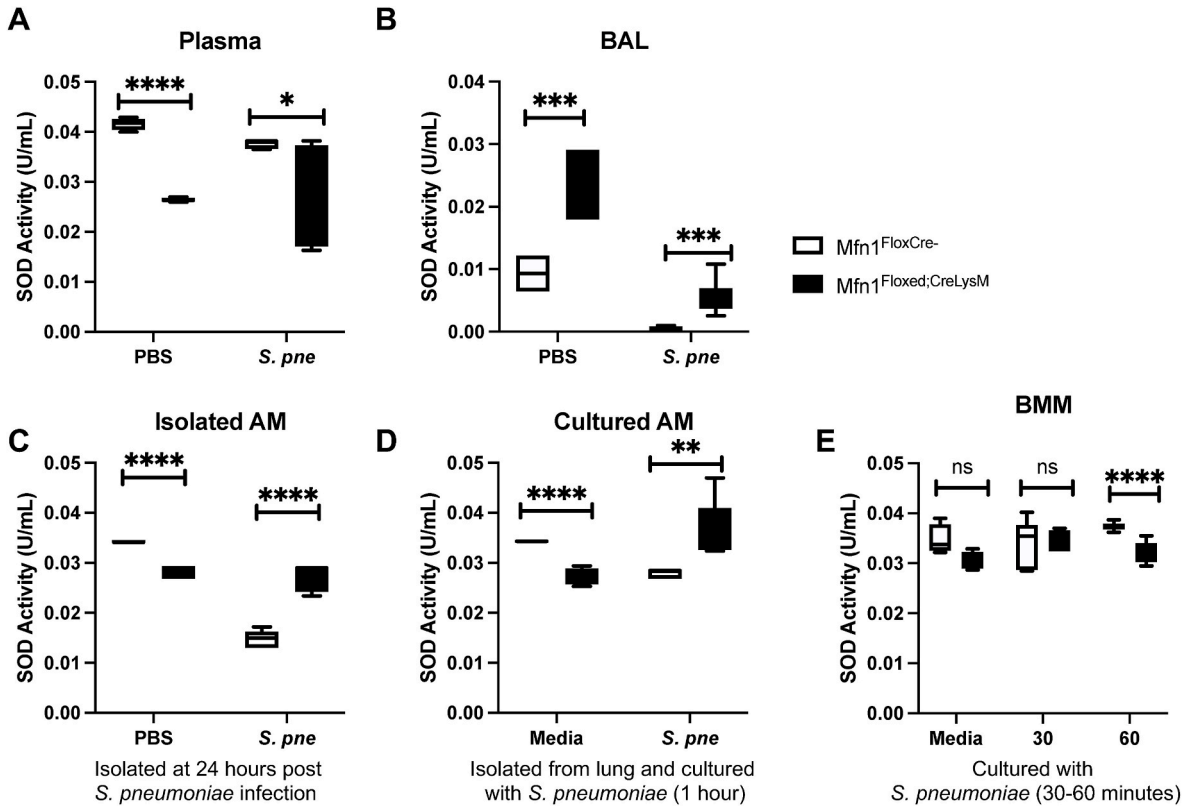

Fig. 7. *Enhanced SOD Activity in Mfn1 Deficient AM during S. pneumoniae Infection.* Wild-type ($Mfn1^{FloxCre-}$) and myeloid deficient Mfn1 ($Mfn1^{Floxed;CreLysM}$) mice were intranasally instilled with 1×10^5 CFU of *S. pneumoniae*. SOD activity was quantified in (A) plasma and (B) bronchoalveolar lavage (BAL) at 24 h post-infection. (C) Alveolar macrophages were isolated from wild-type and Mfn1 deficient AM at 24 h post-PBS or *S. pneumoniae* instillation and SOD activity was assessed. (D) Alveolar macrophages were isolated from naïve wild-type and Mfn1 deficient mice before infection with *S. pneumoniae* (MOI = 10) for 1 h *before* quantification of SOD activity. (E) Bone marrow macrophages (BMM) were isolated from naïve wild-type and Mfn1 deficient mice and infected with *S. pneumoniae* (MOI = 10) for 30–60 min before quantification of SOD activity. Statistical significance was determined for results from independent biological replicates. N = 5–10 samples per group. ns: not significant, $^{**}p < 0.01$, $^{***}p < 0.001$, $^{****}p < 0.0001$. Results were repeated at least three times. Representative results are shown.

wild-type (Fig. 7B). To investigate the role of Mfn1 on SOD activity in AM during *in vivo* infection, we isolated AM from control and *S. pneumoniae*-infected wild-type and Mfn1 deficient mice at 24 h. During *S. pneumoniae*, there was a significant increase in SOD activity quantified in Mfn1 deficient AM (Fig. 7C). We next evaluated the impact of Mfn1 expression in AM on SOD activity in response to direct *S. pneumoniae* infection. To this extent, AMs were isolated from wild-type and Mfn1 deficient mice and cultured with *S. pneumoniae* for 1-h post-binding and gentamicin treatment. Despite lower levels of SOD activity at baseline, there was a significant upregulation in activity in Mfn1 deficient AM that occurred in response to *S. pneumoniae* (Fig. 7D). Using bone marrow-derived macrophages (BMM), we next investigated if Mfn1-mediated changes in SOD activity were unique to AM. When compared to wild-type, there was a significant decrease in SOD activity detected in Mfn1 deficient BMM in response to *S. pneumoniae* (Fig. 7E).

2.7. Mfn1 deficient alveolar macrophages have decreased baseline DNA and RNA oxidation

High levels of ROS can contribute to oxidative damage of DNA and RNA. As guanine has the lowest redox potential, it is the base most susceptible to oxidation [17]. Three oxidized guanine species (OGS) are released when repair processes are initiated to correct the damage: 8-hydroxy-2′-deoxyguanosine (8-OHdG) (from DNA), 8-hydroxyguanosine (8-OHG) (from RNA), and 8-hydroxyguanine (8-OHGua) (from DNA or RNA) [17]. We next evaluated if a deficiency in Mfn1 might contribute to increased DNA and RNA oxidative damage. To this extent, we examined OGS levels in plasma and BAL samples isolated from control (PBS) and *S. pneumoniae*-infected wild-type and myeloid Mfn1 deficient mice at 24 h post-installation. In both plasma and BAL samples, similar levels of OGS were detected in both wild-type and mice with Mfn1 deficient myeloid cells at baseline and during *S. pneumoniae* infection (Fig. 8A–B). To investigate the role of Mfn1 on OGS in AM during *in vivo* infection, we isolated AM from control and *S. pneumoniae*-infected wild-type and myeloid-specific Mfn1 deficient mice at 24 h post-infection. At baseline, there were significantly decreased levels of OGS present in Mfn1 deficient AM compared to wild-type AM (Fig. 8C). No significant difference in OGS was quantified in wild-type and Mfn1 deficient AM in response to *S. pneumoniae* (Fig. 8C). Next, we evaluated the impact of Mfn1 expression in AM on OGS in response to direct *S. pneumoniae* infection. AM were isolated from wild-type and Mfn1 deficient mice and cultured with *S. pneumoniae* for 1-h post-binding and gentamicin treatment. Despite lower levels of OGS at baseline, similar levels were quantified in wild-type and Mfn1 deficient AM in response to *S. pneumoniae* (Fig. 8D). Using bone marrow-derived macrophages (BMM), we next investigated if Mfn1-mediated changes in SOD activity were unique to AM. Compared to the wild-type, in response to *S. pneumoniae*, similar levels of OGS were detected in Mfn1 deficient BMM (Fig. 8E).

2.8. Decreased lipid peroxidation in AM in the Absence of Mfn1

Lipid peroxidation is a mechanism of cellular injury and can indicate oxidative stress within cells and tissues formed as a by-product of lipid peroxidation. Malondialdehyde (MDA) is a naturally occurring product of lipid peroxidation that reacts with thiobarbituric acid (TBA) to form

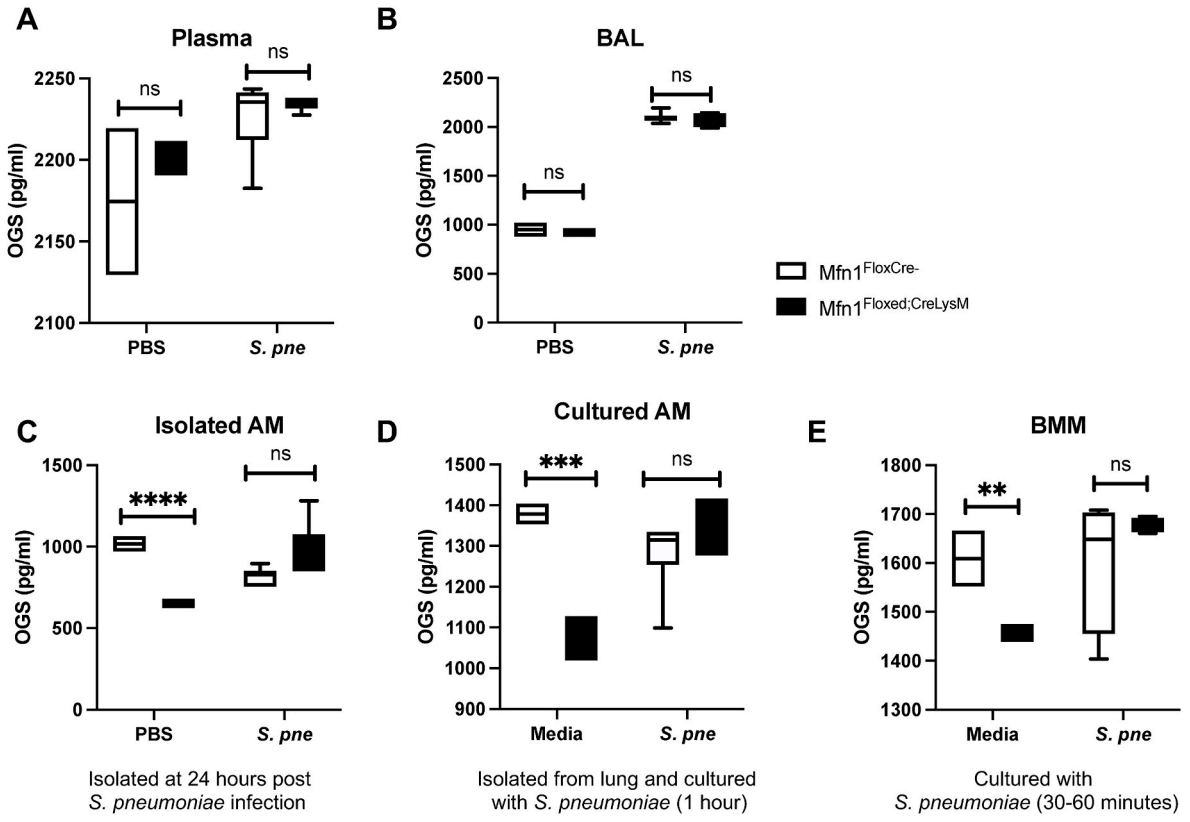

Fig. 8. *Mfn1 Deficient Alveolar Macrophages Have Decreased DNA and RNA Oxidation at 24 h of S. pneumoniae Infection.* Wild-type ($Mfn1^{FloxCre-}$) and myeloid deficient Mfn1 ($Mfn1^{Floxed;CreLysM}$) mice were intranasally instilled with 1×10^5 CFU of *S. pneumoniae*. Oxidized guanine species (OGS) (8-hydroxy-2′-deoxyguanosine (8-OHdG), 8-hydroxyguanosine (8-OHG), and 8-hydroxyguanine (8-OHGua)) were quantified in (**A**) plasma and (**B**) bronchoalveolar lavage (BAL) at 24 h post-infection. (**C**) Alveolar macrophages were isolated from wild-type and Mfn1 deficient AM at 24 h post-PBS or *S. pneumoniae* instillation and OGS levels were assessed. (**D**) Alveolar macrophages were isolated from naïve wild-type and Mfn1 deficient mice before infection with *S. pneumoniae* (MOI = 10) and quantification of OGS levels. (**E**) Bone marrow macrophages (BMM) were isolated from naïve wild-type and Mfn1 deficient mice and infected with *S. pneumoniae* (MOI = 10) for 30–60 min *before* quantification of OGS levels. Statistical significance was determined for results from independent biological replicates. N = 5–10 samples per group. ns: not significant, $^{**}p < 0.01$, $^{***}p < 0.001$, $^{****}p < 0.0001$. Results were repeated at least three times. Representative results are shown.

thiobarbituric acid reactive substances (TBARS) that can be used to quantify lipid peroxidation. Using the TBARS assay, we investigated the impact of an Mfn1 deficiency on lipid peroxidation during *S. pneumoniae* infection. To this extent, we examined lipid peroxidation in plasma and bronchoalveolar lavage (BAL) samples isolated from control (PBS) and *S. pneumoniae*-infected wild-type and Mfn1 deficient mice at 24 h post-instillation. In plasma samples, significantly less lipid peroxidation was detected in mice with Mfn1 deficient myeloid cells at baseline and during *S. pneumoniae* infection (Fig. 9A). We next investigated lipid peroxidation in BAL isolated from wild-type and Mfn1-deficient mice. In response to *S. pneumoniae*, significantly less lipid peroxidation was quantified in BAL collected from Mfn1 deficient mice than in wild-type (Fig. 9B). We next evaluated the impact of Mfn1 expression in AM on lipid peroxidation in response to direct *S. pneumoniae* infection. To this extent, AMs were isolated from wild-type and Mfn1 deficient mice and cultured with *S. pneumoniae* for 1-h post-binding and gentamicin treatment. Despite similar lipid peroxidation levels at baseline, a significant decrease in MDA was quantified in Mfn1 deficient AM in response to *S. pneumoniae* (Fig. 9C). Using bone marrow-derived macrophages (BMM), we next investigated if Mfn1-mediated changes in lipid peroxidation were unique to AM. Similar to results obtained in AM, when compared to wild-type, in response to *S. pneumoniae*, there was a significant decrease in lipid peroxidation detected in Mfn1 deficient BMM (Fig. 9D).

Lipid droplets are important in regulating lipid metabolism and storage and can release unsaturated fatty acids to protect cells from lipid peroxidation [18]. Specifically, the channeling and sequestration of polyunsaturated fatty acids (PUFAs) into lipid droplets has been demonstrated to protect cells from oxidative stress and lipid peroxidation [18]. As lipid peroxidation was significantly decreased in Mfn1 deficient AM, we next investigated the role of Mfn1 in mediating lipid droplet formation in response to *S. pneumoniae*. Despite similar levels at baseline, a significant decrease in lipid droplet formation was quantified in Mfn1 deficient AM compared to wild-type AM when cultured with *S. pneumoniae* (Fig. 9E).

2.9. Antioxidant capacity in BAL is enhanced in Mfn1 deficient mice during S. pneumoniae

Host antioxidant systems, which include enzymes such as SOD, macromolecules such as ferritin, and small molecules such as ascorbic acid, help to circumvent the harmful effects of ROS. To investigate the role of Mfn1 in mediating antioxidant responses, we quantified the combined activity of aqueous and lipid-soluble antioxidants to inhibit 2,2′-Azino-di-[3-ethylbenzthiazoline sulphonate] (ABTS) oxidation by metomyoglobin to $ABTS^+$ [19–21]. Using the antioxidant assay, we investigated the impact of a Mfn1 deficiency on antioxidant capacity during *S. pneumoniae* infection. To this extent, we examined antioxidant levels in plasma and bronchoalveolar lavage (BAL) samples isolated from control (PBS) and *S. pneumoniae*-infected wild-type and Mfn1 deficient mice at 24 h post-installation. In plasma samples, a significant increase in antioxidant capacity was observed in mice with myeloid-specific deficiency in Mfn1 (Fig. 10A). In response to *S. pneumoniae*, antioxidant levels in plasma were significantly enhanced

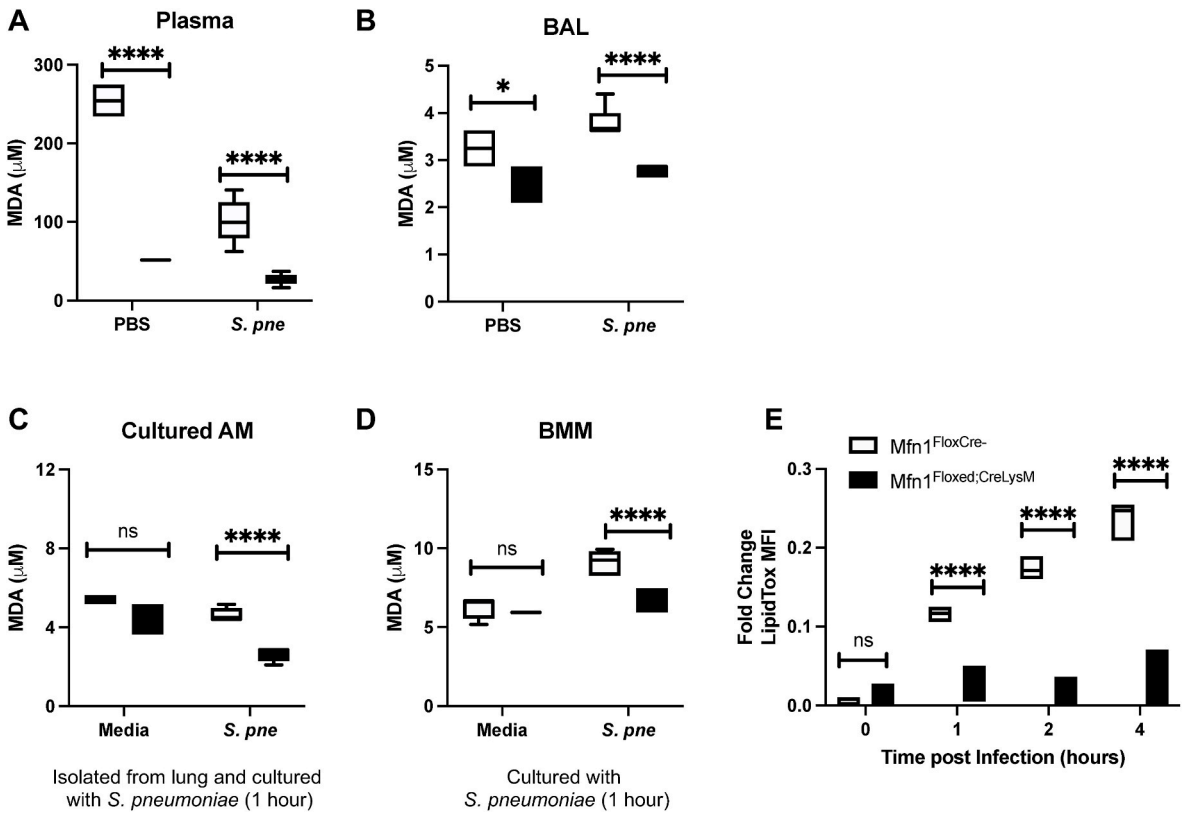

Fig. 9. *Decreased Lipid Peroxidation in AM in the Absence of Mfn1.* Wild-type ($Mfn1^{FloxCre-}$) and myeloid deficient Mfn1 ($Mfn1^{Floxed;CreLysM}$) mice were intranasally instilled with 1×10^5 CFU of *S. pneumoniae*. Lipid peroxidation, as assessed by quantification of malondialdehyde (MDA) by TBARS assay, was performed using (**A**) plasma and (**B**) bronchoalveolar lavage (BAL) at 24 h post-infection. (**C**) Alveolar macrophages were isolated from wild-type and Mfn1 deficient AM at 24 h post-PBS or *S. pneumoniae* instillation and MDA levels were assessed. (**D**) Alveolar macrophages were isolated from naïve wild-type and Mfn1 deficient mice before infection with *S. pneumoniae* (MOI = 10) and quantification of MDA concentration. (**E**) Bone marrow macrophages (BMM) were isolated from naïve wild-type and Mfn1 deficient mice and infected with *S. pneumoniae* (MOI = 10) for 30–60 min before MDA quantification. Statistical significance was determined for results from independent biological replicates. N = 5–10 samples per group. ns: not significant, $^*p < 0.05$, $^{****}p < 0.0001$. Results were repeated at least three times. Representative results are shown.

in wild-type mice, with higher levels than Mfn1 deficient mice (Fig. 10A). Next, we investigated antioxidant activity in BAL isolated from wild-type and Mfn1-deficient mice. At baseline and in response to *S. pneumoniae*, significantly enhanced antioxidant levels were quantified in BAL collected from Mfn1 deficient mice compared to wild-type (Fig. 10B). Next, we evaluated the impact of Mfn1 expression in AM on antioxidant levels in response to direct *S. pneumoniae* infection. To this extent, AMs were isolated from wild-type and Mfn1 deficient mice and cultured with *S. pneumoniae* for 1-h post-binding and gentamicin treatment. Similar levels of antioxidant activity were observed in wild-type and Mfn1 deficient AM at baseline and during infection (Fig. 10C). Using bone marrow-derived macrophages (BMM), we next investigated if Mfn1-mediated changes in antioxidant activity were unique to AM. Compared to wild-type, similar antioxidant levels were quantified in Mfn1 deficient BMM (Fig. 10D).

3. Discussion

Results of our study demonstrate that Mfn1 plays an essential role in mediating lipid peroxidation and superoxide dismutase (SOD) activity in alveolar macrophages during *S. pneumoniae*.

Mitochondrial fusion proteins, Mfn1 and Mfn2, possess GTP binding activity and are located on the outer mitochondrial membrane but have distinct roles in mediating host responses. While Mfn1 is responsible for mitochondria tethering and mitochondrial responses to oxidative stress, Mfn2 plays a vital role in controlling the shape of ER and mitochondrial-associated membrane (MAM)-mediated ER-mitochondrial interactions [22–24]. Mfn2 is enriched in MAM and localizes on the ER, where it can interact with Mfn 1 or 2 present on the outer mitochondrial membrane (OMM) to form a bridge between the organelles [22,25]. Recent work has demonstrated that Mfn2 is crucial in mediating normal glucose homeostasis and insulin signaling [26,27]. Without Mfn2, there was increased ER stress, enhanced hydrogen peroxide levels, and altered ROS signaling [27]. Hepatic deletion of Mfn1 resulted in mitochondrial network fragmentation, increased mitochondrial respiratory capacity, increased ROS production, and led to using lipids as a primary energy source [28]. Importantly, liver-specific knockdown of Mfn1 protected mice against high-fat diet-induced insulin resistance [28].

In response to TLR stimulatory ligands, LPS, CpG-B, and R848, and cytokines, such as IFN-γ and IL-4, Mfn2 expression was induced in bone marrow-derived macrophages [29]. These results demonstrated that Mfn2 was critical in mediating macrophage responses when large amounts of ROS are required, with pro-inflammatory and phagocytic responses being impaired in myeloid cells lacking Mfn2 [29]. Importantly, these studies demonstrated that despite increased mitochondrial fragmentation, mitochondrial ROS was not altered in Mfn1 deficient cells compared to controls [29]. In agreement with these findings, we observed that mitochondrial ROS in wild-type and Mfn1 deficient bone marrow-derived macrophages were similar (data not shown). Interestingly, despite similar cellular ROS levels at baseline, significantly lower mitochondrial ROS levels were observed in freshly isolated Mfn1 deficient AM when compared to wild-type. Cellular adaptations to ROS production might contribute to protecting Mfn1-deficient mitochondria against ROS damage and may be unique to the tissue environment. We

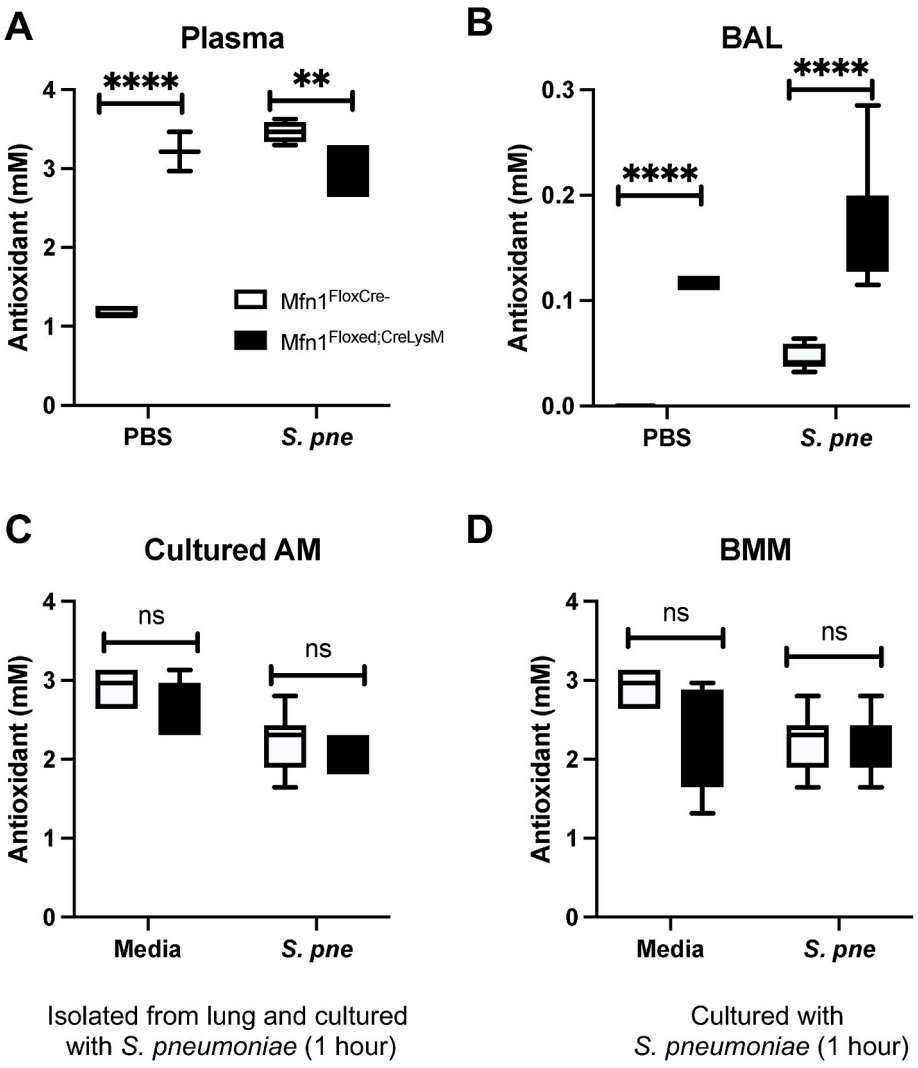

Fig. 10. *Enhanced Antioxidant Capacity in Mfn1 Deficient BAL during S. pneumoniae.* Wild-type ($Mfn1^{FloxCre-}$) and myeloid deficient Mfn1 ($Mfn1^{Floxed;CreLysM}$) mice were intranasally instilled with 1×10^5 CFU of *S. pneumoniae*. Total antioxidant concentration was assessed in (**A**) plasma and (**B**) bronchoalveolar lavage (BAL) at 24 h post-infection. (**C**) Alveolar macrophages were isolated from naïve wild-type and Mfn1 deficient mice before infection with *S. pneumoniae* (MOI = 10) and quantification of antioxidant concentration. (**D**) Bone marrow macrophages (BMM) were isolated from naïve wild-type and Mfn1 deficient mice and infected with *S. pneumoniae* (MOI = 10) for 30–60 min before antioxidant quantification. Statistical significance was determined for results from independent biological replicates. N = 5–10 samples per group. ns: not significant, $^{**}p < 0.01$, $^{****}p < 0.0001$. Results were repeated at least three times. Representative results are shown.

observed a significant increase in antioxidant and SOD activity present in BAL collected from Mfn1-deficient mice. While we did not observe a difference in antioxidant activity in cultured alveolar macrophages, in the absence of Mfn1, there was decreased baseline SOD activity. In response to *S. pneumoniae*, SOD activity remained elevated in Mfn1-deficient AM. Our results, in agreement with previously published studies, demonstrate that baseline mitochondrial bioenergetics, specifically basal respiration and ATP production, were significantly decreased in Mfn1 deficient AM [30]. In the absence of Mfn1, decreased mitochondrial ROS due to diminished proton leak may contribute to lower SOD activity at baseline. However, during *S. pneumoniae,* it is possible that in response to other mitochondrial enzyme complexes, such as dihydrolipoamide dehydrogenase-containing FAD-linked pyruvate and the electron-transferring flavoprotein: Q oxidoreductase (ETFQOR) of fatty acid β-oxidation may contribute to ROS production and subsequent generation of superoxide [31,32].

Notably, previous studies have highlighted a key role for Mfn2 but not Mfn1 in protecting mice from *Listeria monocytogenes*, *Mycobacterium tuberculosis*, and LPS endotoxemia [29]. In the absence of Mfn2, changes in mitochondrial morphology may contribute to decreased ER-mitochondrial communication and alterations in lipid transport within the cell [25,33,34]. Our results demonstrate decreased *S. pneumoniae*-induced chemokine and cytokine production in lung and AM isolated from Mfn1 deficient mice. Previous work has illustrated that SIMH promotes NF-κB activation [35]. In response to *S. pneumoniae*, increased cellular recruitment and lung tissue injury were observed in wild-type mice. In the absence of Mfn1, it is possible that decreased NF-κB mediated chemokine and cytokine production contributed to decreased inflammatory cell recruitment. Despite decreased immune cell infiltration, increased bacterial clearance was observed in the absence of Mfn1. It is possible that a differential immune signaling cascade occurred in the Mfn1 deficient AM, in which enhanced SOD activity and elevated hydrogen peroxide production aid in bacterial clearance by resident AM. Changes in SOD activity, significant upregulation of several phagocytic receptors, and Mfn1 deficient AM may further contribute to enhanced *S. pneumoniae* clearance. Importantly, as Mfn1 2 is essential for SIMH induction, it is plausible that there may be different macrophage requirements for SIMH to sustain mitochondrial bioenergetics and cell survival in response to different infectious stimuli.

Of note, Mfn1 deficient alveolar and bone marrow-derived

macrophages have decreased DNA/RNA oxidation. However, in response to *S. pneumoniae*, DNA/RNA oxidation was elevated to similar levels between wild-type and Mfn1 deficient macrophages. Decreased baseline levels of OGS were associated with lower mitochondrial ROS and SOD activity. Previous work has demonstrated that Mfn1 deletion improves the tolerance of cardiomyocytes to ROS-induced mitochondrial dysfunction [36]. Deleting Mfn1 may contribute to changes in ROS and oxidative DNA/RNA damage. However, in response to *S. pneumoniae*, these systems cannot prevent ROS-induced damage in macrophages. Our data demonstrate that in the absence of Mfn1, innate immune responses to *S. pneumoniae* are significantly dysregulated. Despite low ROS production, elevated DNA/RNA oxidation was observed in Mfn1-deficient macrophages. This data indicated that oxidative stress impacting DNA/RNA oxidation was not the primary driver of the enhanced host defense observed in Mfn1-deficient macrophages. Instead, our findings highlight the possibility that other oxidative mechanisms, such as lipid peroxidation, play a more significant role in bacterial clearance.

Decreased injury to Mfn1 deficient lungs was associated with reduced cellular infiltration and diminished pro-inflammatory cytokine production. Our results also show that mitochondrial ROS levels were significantly lower in Mfn1 deficient macrophages in response to direct infection with *S. pneumoniae*. It is possible that due to increased mitochondrial rupture that occurs in Mfn1 deficient macrophages, there was a significant alteration in mitochondrial ROS-mediated innate signaling mechanisms. The relationship between ROS levels and phagocytosis is complex and controversial. The impact can vary depending on the cell type and the context of the immune response [37]. Our results demonstrate two potential mechanisms that may contribute to improved bacterial clearance in Mfn1 deficient lung: 1) a significant increase in phagocytosis receptors in alveolar macrophages in response to direct *S. pneumoniae* infection and 2) enhanced hydrogen peroxide production. It is important to note that the viability of Mfn1 macrophages significantly decreases at later time points of infection.

Polyunsaturated fatty acids (PUFAs) in cellular and organelle membranes are highly susceptible to ROS damage and can undergo lipid peroxidation. Lipid peroxidation can directly damage phospholipids, contributing to increased pro-inflammatory signaling. Specifically, lipid peroxidation products can stimulate NF-kB activity by inhibiting IkB degradation [38]. Additional studies have demonstrated a key role for lipid peroxidation in mediating mitogen-activated protein kinases (MAPK) and protein kinase C (PKC) signaling [38,39]. Importantly, in response to ROS-induced damage of lipids, enzymatic antioxidants like superoxide dismutase (SOD) can counteract free radicals and neutralize oxidants [40]. In the absence of Mfn1, there was decreased lipid peroxidation that was associated with increased SOD activity in alveolar macrophages in response to *S. pneumoniae*. It is possible that due to the inability to undergo SIMH due to diminished Mfn1 expression, enhanced ER stress may mediate the induction of SOD activity as a means to counteract the detrimental effects of mitochondrial stress. Increased SOD activity and subsequent decrease in lipid peroxidation in the absence of Mfn1 may exist as a mechanism that functions to regulate ROS-mediated responses to *S. pneumoniae*.

Recent work using an adenoviral expression system demonstrated that Mfn1 overexpression contributed to metabolic remodeling in pulmonary endothelial cells. In addition, overexpression of Mfn1 increased mitochondrial ROS and disrupted electron transport chain complexes I and III [16]. Importantly, overexpression of Mfn1 promoted mitochondrial fusion and induced metabolic changes in endothelial cells [16]. Our current study was designed to examine the role of diminished Mfn1 expression in myeloid cells, specifically alveolar macrophages, on host responses to *S. pneumoniae*. While our results agree that Mfn1 expression correlates with mitochondrial ROS, our current findings shed light on the consequences of reduced Mfn1 levels within the innate immune cells of the lung. Findings from our current study demonstrate that in the absence of Mfn1, SIMH was decreased. Decreased SIMH enhanced mitochondrial apoptosis in macrophages in response to *S. pneumoniae*. Furthermore, a myeloid-specific knockdown of Mfn1 allowed us to focus on its unique role in mediating host innate immune responses to pathogenic stimuli, such as *S. pneumoniae*.

Notably, antioxidant capacity was significantly elevated in BAL collected from Mfn1 deficient mice at baseline and during *S. pneumoniae*. We did not observe significantly different antioxidant levels in wild-type and Mfn1 deficient macrophages at baseline or during *S. pneumoniae*. Elevated antioxidant levels in the BAL may be specific to the site of infection and contribute to decreased pro-inflammatory responses and tissue injury. Recent work has demonstrated that capillary leakage during primary influenza infection provides nutrients and antioxidants that counteract oxidative damage and aid in the proliferation of *S. pneumoniae* [41]. Specifically, pneumococcal adaptation to influenza-induced inflammation and redox imbalance increased bacterial load, decreased opsonophagocytosis, and increased stress adaptation [41]. Due to the increased antioxidant levels present in Mfn1 deficient BAL, it might be possible that increased clearance of *S. pneumoniae* may be due to an inability to adapt to the host lung environment. The impact of primary influenza infection on these parameters and S. pneumoniae adaptation will need to be pursued in future avenues of study.

4. Materials and methods

4.1. Mice

Mfn1$^{loxp/loxp}$ (029901-UCD) were generated by Dr. David C. Chan (California Institute of Technology, Pasadena, CA) and purchased from Mutant Mouse Resource & Research Center (University of California, Davis, CA). Myeloid-specific *Mfn1* gene single-knockout strain was generated by crossing *Mfn1*$^{loxp/loxp}$ (*Mfn1*$^{fl/fl}$) to (*LysM-Cre* strain; 004781, Jackson Laboratory, Bar Harbor, ME) to produce *Mfn1*$^{fl/fl}$*LysM-Cre*$^{+/-}$ (Mfn1$^{\text{Floxed; CreLysM}}$) [42]. Wild-type controls used for comparison were *Mfn1*$^{fl/fl}$*LysM-Cre*$^{-/-}$ (Mfn1$^{\text{FloxCre}-}$) mice. Age-matched male and female Mfn1$^{\text{FloxCre}-}$ and Mfn1$^{\text{Floxed; CreLysM}}$ were bred in the WCM animal facility. Mice received identical husbandry conditions. The IACUC at Weill Cornell Medicine approved the use of animals in this study, and methods were carried out following the relevant guidelines and regulations. Mice were used at 3 months of age.

4.2. Streptococcus pneumoniae

Serotype 3 strain ATCC 6303 (American Type Culture Collection) was used using previously published methods [2].

4.3. Cell culture

Alveolar macrophages (AM) were isolated from freshly isolated lung tissue as previously described [2]. Siglec F$^+$ CD64$^+$ CD11c$^+$ CD11b$^-$ AM populations were allowed to rest for 1 h or overnight (Seahorse analysis) before each experiment. Bone marrow-derived macrophages (BMM) were generated using previously published methods [43–45]. On day 7 of culture, BMM were replated (1×10^6 cells/ml) 24 h before infection or stimulation.

4.4. In vitro assays

DNA/RNA oxidative damage (high sensitivity) (catalog #: 589320), ROS detection cell-based assay kit (catalog #: 601290), superoxide dismutase assay kit (catalog #: 706002), TBARS assay kit (catalog #: 10009055), hydrogen peroxide (catalog #: 6000050), mitochondrial ROS detection assay kit (catalog #: 701600), and antioxidant assay kit (catalog #: 709001) were purchased from Cayman Chemical (Ann Arbor, MI). LipidTOX Deep Red Neutral Lipid Stain (ThermoFisher Scientific, catalog #: H34477) was utilized to assess lipid droplet

formation. All assays were performed in triplicate per manufacturers' protocols.

4.5. Mitochondrial bioenergetic measurements

The Seahorse XF Mito Stress Test was used to measure the mitochondrial respiration rate (catalog #: 103015-100, Agilent Technologies, Wilmington, DE). Using previously published methods, sequential injection of oligomycin (1.0 μM), carbonyl cyanide-4-(trifluoromethoxy) phenylhydrazone (FCCP) (1.0 μM for BMDMs and 4.0 μM for AMs), and rotenone/antimycin A (1.0 μM) [46]. Cells were plated 4x104 overnight in DMEM containing 20 % L929 media and equilibrated in XF DMEM base media (catalog #: 103575-100) supplemented with 10 mM glucose (catalog #: 103577-100), 2 mM L-glutamine (catalog #: 103579-100), and 1 mM sodium pyruvate (catalog #: 103578-100) at 37 °C, no CO_2 for 1 h prior to measurement (Agilent Technologies).

4.6. In vivo procedures and tissue collection

Streptococcus pneumoniae infection: All mice were instilled intranasally with PBS or 1×10^5 CFU of *S. pneumoniae* (50-μL volume in PBS) [2]. *Bronchoalveolar lavage (BAL):* BAL was collected using previously published methods [2,47]. *Bacterial titer assay of lung tissue*: Lung tissue samples were homogenized before serial dilution in THB [2]. *Lung permeability assay*: Mice received 50-μL of FITC-Dextran (3 mg/kg: intranasally), and fluorescence was measured in plasma at 1-h post-instillation [2]. *Histology:* The whole lung was distended with 1 % low melting agarose and placed into cold formalin to maintain architecture [48]. Tissue samples were processed by the Translational Research Program at WCM Pathology and Laboratory of Medicine. Images were scanned using the EVOS FL Auto Imaging System (ThermoFisher Scientific, Waltham, MA, USA).

4.7. RNA purification and real-time PCR

RNA samples were extracted using the automated Maxwell RNA extraction protocol (Madison, WI, USA). Samples were reverse transcribed using the First Stand Synthesis Kit and quantified with RT^2 Profiler™ Assays (Qiagen, PAMM-148Z, PAMM-173Z, and PAMM-089Z). PCR efficiency, reproducibility, and expression were evaluated using online analytical software provided by Qiagen Gene Globe.

4.8. Cytokine quantification in lung tissue

Lung tissue samples were processed and quantified using the mouse XL Cytokine Array Kit (R&D Systems) as previously described [2].

4.9. Transmission electron microscopy (TEM)

TEM sample preparation was performed as previously described [2]. Cells were washed with PBS before the addition of TEM fixative. Samples were submitted to the WCM Microscopy and Image Analysis Core Facility for sample processing and image acquisition. Images were obtained with a Jeol electron microscope (JEM-1400) with an accelerating voltage of 100 kV.

4.10. Protein isolation and western blotting

Protein was isolated from alveolar macrophages using the Minute Total Protein Extraction Kit (Invent Technologies). Total protein content (10 μg total protein) was used for western blotting. Total OXPHOS rodent antibody cocktail (catalog#: ab110413) (Abcam, Boston MA) and Tom20 (catalog#: 42406S) (Cell Signaling Technology, Danvers MA) were used for western blot analysis. Images were acquired on film or using the Azure 300 imaging system (Azure Biosystems, Dublin, CA).

4.11. Statistical analysis

Survival analysis between groups was calculated using the Mantel-Cox test. A comparison of groups was performed using a two-tailed *t*-test, and comparisons between groups were verified using one-way ANOVA. All samples were independent, and statistical significance was determined for results from independent biological replicates. The sample size was at least N = 3 for *in vitro* experiments and N = 5–10 for *in vivo* experiments. All data were analyzed using GraphPad Prism software (San Diego, CA, USA). Statistical significance was considered by a * $p < 0.05$, ** $p < 0.01$, *** $p < 0.001$, and **** $p < 0.0001$.

CRediT authorship contribution statement

David Thomas: Conceptualization, Data curation, Methodology, Writing – original draft, Writing – review & editing. **Jianjun Yang:** Data curation, Formal analysis. **Soo Jung Cho:** Conceptualization, Formal analysis, Writing – original draft, Writing – review & editing. **Heather Stout-Delgado:** Conceptualization, Data curation, Formal analysis, Funding acquisition, Methodology, Supervision, Writing – original draft, Writing – review & editing.

Declaration of competing interest

The authors declare that they have no known competing financial interests or personal relationships that could have appeared to influence the work reported in this paper.

Appendix A. Supplementary data

Supplementary data to this article can be found online at https://doi.org/10.1016/j.redox.2024.103329.

References

[1] A. Ortqvist, J. Hedlund, M. Kalin, Streptococcus pneumoniae: epidemiology, risk factors, and clinical features, Semin. Respir. Crit. Care Med. 26 (6) (2005) 563–574.
[2] S.J. Cho, A. Pronko, J. Yang, K. Pagan, H. Stout-Delgado, Role of cholesterol 25-hydroxylase (Ch25h) in mediating innate immune responses to Streptococcus pneumoniae infection, Cells 12 (4) (2023).
[3] A.P. West, I.E. Brodsky, C. Rahner, D.K. Woo, H. Erdjument-Bromage, P. Tempst, et al., TLR signalling augments macrophage bactericidal activity through mitochondrial ROS, Nature 472 (7344) (2011) 476–480.
[4] L.A. O'Neill, E.J. Pearce, Immunometabolism governs dendritic cell and macrophage function, J. Exp. Med. 213 (1) (2016) 15–23.
[5] A. Zahedi, R. Phandthong, A. Chaili, S. Leung, E. Omaiye, P. Talbot, Mitochondrial stress response in neural stem cells exposed to electronic cigarettes, iScience 16 (2019) 250–269.
[6] J. Lebeau, J.M. Saunders, V.W.R. Moraes, A. Madhavan, N. Madrazo, M. C. Anthony, et al., The PERK arm of the unfolded protein response regulates mitochondrial morphology during acute endoplasmic reticulum stress, Cell Rep. 22 (11) (2018) 2827–2836.
[7] D. Tondera, S. Grandemange, A. Jourdain, M. Karbowski, Y. Mattenberger, S. Herzig, et al., SLP-2 is required for stress-induced mitochondrial hyperfusion, EMBO J. 28 (11) (2009) 1589–1600.
[8] W. Qian, S. Choi, G.A. Gibson, S.C. Watkins, C.J. Bakkenist, B. Van Houten, Mitochondrial hyperfusion induced by loss of the fission protein Drp1 causes ATM-dependent G2/M arrest and aneuploidy through DNA replication stress, J. Cell Sci. 125 (Pt 23) (2012) 5745–5757.
[9] M.O. Abdullah, R.X. Zeng, C.L. Margerum, D. Papadopoli, C. Monnin, K.B. Punter, et al., Mitochondrial hyperfusion via metabolic sensing of regulatory amino acids, Cell Rep. 40 (7) (2022) 111198.
[10] T. Shutt, M. Geoffrion, R. Milne, H.M. McBride, The intracellular redox state is a core determinant of mitochondrial fusion, EMBO Rep. 13 (10) (2012) 909–915.
[11] P.H. Willems, R. Rossignol, C.E. Dieteren, M.P. Murphy, W.J. Koopman, Redox homeostasis and mitochondrial dynamics, Cell Metabol. 22 (2) (2015) 207–218.
[12] C. Castanier, D. Garcin, A. Vazquez, D. Arnoult, Mitochondrial dynamics regulate the RIG-I-like receptor antiviral pathway, EMBO Rep. 11 (2) (2010) 133–138.
[13] K. Onoguchi, K. Onomoto, S. Takamatsu, M. Jogi, A. Takemura, S. Morimoto, et al., Virus-infection or 5'ppp-RNA activates antiviral signal through redistribution of IPS-1 mediated by MFN1, PLoS Pathog. 6 (7) (2010) e1001012.
[14] K. Huang, S. Pei, Y. Sun, X. Xu, Y. Fang, M. Lai, et al., Mitofusin 1-mediated redistribution of mitochondrial antiviral signaling protein promotes type 1

interferon response in human cytomegalovirus infection, Microbiol. Spectr. 11 (2) (2023) e0461522.
[15] A.L. McCubbrey, K.C. Allison, A.B. Lee-Sherick, C.V. Jakubzick, W.J. Janssen, Promoter specificity and efficacy in conditional and inducible transgenic targeting of lung macrophages, Front. Immunol. 8 (2017) 1618.
[16] M. Yegambaram, X. Sun, A.G. Flores, Q. Lu, J. Soto, J. Richards, et al., Novel relationship between mitofusin 2-mediated mitochondrial hyperfusion, metabolic remodeling, and glycolysis in pulmonary arterial endothelial cells, Int. J. Mol. Sci. 24 (24) (2023).
[17] K. Kino, M. Hirao-Suzuki, M. Morikawa, A. Sakaga, H. Miyazawa, Generation, repair and replication of guanine oxidation products, Gene Environ. 39 (2017) 21.
[18] M. Danielli, L. Perne, E. Jarc Jovicic, T. Petan, Lipid droplets and polyunsaturated fatty acid trafficking: balancing life and death, Front. Cell Dev. Biol. 11 (2023) 1104725.
[19] N.J. Miller, C. Rice-Evans, M.J. Davies, A new method for measuring antioxidant activity, Biochem. Soc. Trans. 21 (2) (1993) 95S.
[20] N.J. Miller, C. Rice-Evans, M.J. Davies, V. Gopinathan, A. Milner, A novel method for measuring antioxidant capacity and its application to monitoring the antioxidant status in premature neonates, Clin Sci (Lond). 84 (4) (1993) 407–412.
[21] N.J. Miller, C.A. Rice-Evans, Factors influencing the antioxidant activity determined by the ABTS.+ radical cation assay, Free Radic. Res. 26 (3) (1997) 195–199.
[22] O.M. de Brito, L. Scorrano, Mitofusin 2 tethers endoplasmic reticulum to mitochondria, Nature 456 (7222) (2008) 605–610.
[23] O.M. de Brito, L. Scorrano, Mitofusin 2: a mitochondria-shaping protein with signaling roles beyond fusion, Antioxidants Redox Signal. 10 (3) (2008) 621–633.
[24] R. Filadi, E. Greotti, G. Turacchio, A. Luini, T. Pozzan, P. Pizzo, On the role of Mitofusin 2 in endoplasmic reticulum-mitochondria tethering, Proc. Natl. Acad. Sci. U.S.A. 114 (12) (2017) E2266–E2267.
[25] O.M. de Brito, L. Scorrano, Mitofusin-2 regulates mitochondrial and endoplasmic reticulum morphology and tethering: the role of Ras, Mitochondrion 9 (3) (2009) 222–226.
[26] M.I. Hernandez-Alvarez, D. Sebastian, S. Vives, S. Ivanova, P. Bartoccioni, P. Kakimoto, et al., Deficient endoplasmic reticulum-mitochondrial phosphatidylserine transfer causes liver disease, Cell 177 (4) (2019) 881–895 e17.
[27] D. Sebastian, M.I. Hernandez-Alvarez, J. Segales, E. Sorianello, J.P. Munoz, D. Sala, et al., Mitofusin 2 (Mfn2) links mitochondrial and endoplasmic reticulum function with insulin signaling and is essential for normal glucose homeostasis, Proc. Natl. Acad. Sci. U.S.A. 109 (14) (2012) 5523–5528.
[28] S.S. Kulkarni, M. Joffraud, M. Boutant, J. Ratajczak, A.W. Gao, C. Maclachlan, et al., Mfn1 deficiency in the liver protects against diet-induced insulin resistance and enhances the hypoglycemic effect of metformin, Diabetes 65 (12) (2016) 3552–3560.
[29] J. Tur, S. Pereira-Lopes, T. Vico, E.A. Marin, J.P. Munoz, M. Hernandez-Alvarez, et al., Mitofusin 2 in macrophages links mitochondrial ROS production, cytokine release, phagocytosis, autophagy, and bactericidal activity, Cell Rep. 32 (8) (2020) 108079.
[30] J.M. Son, E.H. Sarsour, A. Kakkerla Balaraju, J. Fussell, A.L. Kalen, B.A. Wagner, et al., Mitofusin 1 and optic atrophy 1 shift metabolism to mitochondrial respiration during aging, Aging Cell 16 (5) (2017) 1136–1145.
[31] J. St-Pierre, J.A. Buckingham, S.J. Roebuck, M.D. Brand, Topology of superoxide production from different sites in the mitochondrial electron transport chain, J. Biol. Chem. 277 (47) (2002) 44784–44790.
[32] A.A. Starkov, G. Fiskum, C. Chinopoulos, B.J. Lorenzo, S.E. Browne, M.S. Patel, et al., Mitochondrial alpha-ketoglutarate dehydrogenase complex generates reactive oxygen species, J. Neurosci. 24 (36) (2004) 7779–7788.
[33] E.A. Schon, E. Area-Gomez, Mitochondria-associated ER membranes in Alzheimer disease, Mol. Cell. Neurosci. 55 (2013) 26–36.
[34] E. Area-Gomez, M. Del Carmen Lara Castillo, M.D. Tambini, C. Guardia-Laguarta, A.J. de Groof, M. Madra, et al., Upregulated function of mitochondria-associated ER membranes in Alzheimer disease, EMBO J. 31 (21) (2012) 4106–4123.
[35] N. Zemirli, M. Pourcelot, G. Ambroise, E. Hatchi, A. Vazquez, D. Arnoult, Mitochondrial hyperfusion promotes NF-kappaB activation via the mitochondrial E3 ligase MULAN, FEBS J. 281 (14) (2014) 3095–3112.
[36] K.N. Papanicolaou, G.A. Ngoh, E.R. Dabkowski, K.A. O'Connell, R.F. Ribeiro Jr., W. C. Stanley, et al., Cardiomyocyte deletion of mitofusin-1 leads to mitochondrial fragmentation and improves tolerance to ROS-induced mitochondrial dysfunction and cell death, Am. J. Physiol. Heart Circ. Physiol. 302 (1) (2012) H167–H179.
[37] C.N. Paiva, M.T. Bozza, Are reactive oxygen species always detrimental to pathogens? Antioxidants Redox Signal. 20 (6) (2014) 1000–1037.
[38] S. Page, C. Fischer, B. Baumgartner, M. Haas, U. Kreusel, G. Loidl, et al., 4-Hydroxynonenal prevents NF-kappaB activation and tumor necrosis factor expression by inhibiting IkappaB phosphorylation and subsequent proteolysis, J. Biol. Chem. 274 (17) (1999) 11611–11618.
[39] C. Giorgi, C. Agnoletto, C. Baldini, A. Bononi, M. Bonora, S. Marchi, et al., Redox control of protein kinase C: cell- and disease-specific aspects, Antioxidants Redox Signal. 13 (7) (2010) 1051–1085.
[40] L.J. Su, J.H. Zhang, H. Gomez, R. Murugan, X. Hong, D. Xu, et al., Reactive oxygen species-induced lipid peroxidation in apoptosis, autophagy, and ferroptosis, Oxid. Med. Cell. Longev. 2019 (2019) 5080843.
[41] V. Sender, K. Hentrich, A. Pathak, A. Tan Qian Ler, B.T. Embaie, S.L. Lundstrom, et al., Capillary leakage provides nutrients and antioxidants for rapid pneumococcal proliferation in influenza-infected lower airways, Proc. Natl. Acad. Sci. U.S.A. 117 (49) (2020) 31386–31397.
[42] D. Bhatia, A. Capili, K. Nakahira, T. Muthukumar, L.K. Torres, A.M.K. Choi, et al., Conditional deletion of myeloid-specific mitofusin 2 but not mitofusin 1 promotes kidney fibrosis, Kidney Int. 101 (5) (2022) 963–986.
[43] K. Inaba, M. Inaba, N. Romani, H. Aya, M. Deguchi, S. Ikehara, et al., Generation of large numbers of dendritic cells from mouse bone marrow cultures supplemented with granulocyte/macrophage colony-stimulating factor, J. Exp. Med. 176 (6) (1992) 1693–1702.
[44] X. Zhang, R. Goncalves, D.M. Mosser, The isolation and characterization of murine macrophages, in: John E. Coligan, et al. (Eds.), Current Protocols in Immunology, 2008 (Chapter 14):Unit 14 1.
[45] S.J. Cho, K. Rooney, A.M.K. Choi, H.W. Stout-Delgado, NLRP3 inflammasome activation in aged macrophages is diminished during Streptococcus pneumoniae infection, Am. J. Physiol. Lung Cell Mol. Physiol. 314 (3) (2018) L372–L387.
[46] P.S. Woods, L.M. Kimmig, A.Y. Meliton, K.A. Sun, Y. Tian, E.M. O'Leary, et al., Tissue-resident alveolar macrophages do not rely on glycolysis for LPS-induced inflammation, Am. J. Respir. Cell Mol. Biol. 62 (2) (2020) 243–255.
[47] F. Sun, G. Xiao, Z. Qu, Murine bronchoalveolar lavage, Bio Protoc. 7 (10) (2017).
[48] A.C. Halbower, R.J. Mason, S.H. Abman, R.M. Tuder, Agarose infiltration improves morphology of cryostat sections of lung, Lab. Invest. 71 (1) (1994) 149–153.